

Journal of Environmental Science and Technology

ISSN 1994-7887





ISSN 1994-7887 DOI: 10.3923/jest.2018.95.103



Research Article

Radionuclides Distribution in Marine Sediment from Abu Soma Bay, Egyptian Red Sea Coast

¹Atef El-Taher, ²Saleh Alashrah, ³Hashem A. Madkour, ⁴A. Al-Sayed and ⁵Taha M. El-Erian

Abstract

Background and Objective: Measurements of natural radionuclides concentrations (226Ra, 232Th and 40K) in sediments collected from sea, rivers or ocean is significant to protect the sea water ecosystem and to human health from radiation. **Materials and Methods:** Thirty sediment samples were collected from Abu Soma Bay, Red Sea coast, Egypt for investigation by gamma-ray spectrometer using NaI (TI) detector. **Results:** The average activity concentrations of 226Ra, 232Th and 40K were 37.2, 25.7 and 265.5 Bq kg⁻¹. These results were compared with reported ranges in the literature from other location in the world. The radiation hazard parameters, radium equivalent activity annual dose, external hazard were also calculated and compared with the recommended levels by International Commission on Radiological Protection and united nations scientific committee on the effects of atomic radiation UNSCEAR reports. **Conclusion:** According to the obtained results, all samples would not present significant radiological hazards. Because there are no existing databases for the natural radioactivity in the sediment samples along Abu Soma Bay, our results are a start to establish a database for Abu Soma bay environment.

Key words: Abu smoma bay, thirty sediments, natural radionuclides, radium equivalent

Citation: Atef El-Taher, Saleh Alashrah, Hashem A. Madkour, A. Al-Sayed and Taha M. El-Erian, 2018. Radionuclides distribution in marine sediment from abu soma bay, Egyptian red sea coast. J. Environ. Sci. Technol., 11: 95-103.

Corresponding Author: Saleh Alashrah, Department of Physics, Faculty of Science, Qassim University Buraydah, 51452 Buraydah, Kingdom of Saudi Arabia

Copyright: © 2018 Atef El-Taher *et al.* This is an open access article distributed under the terms of the creative commons attribution License, which permits unrestricted use, distribution and reproduction in any medium, provided the original author and source are credited.

Competing Interest: The authors have declared that no competing interest exists.

Data Availability: All relevant data are within the paper and its supporting information files.

¹Department of Physics, Faculty of Science, Al-Azher University, Assuit Branch, 71542 Assuit, Egypt

²Department of Physics, Faculty of Science, Qassim University Buraydah, 51452 Buraydah, Kingdom of Saudi Arabia

³National Institute of Oceanography and Fisheries, Red Sea Branch, 84511 Hurghada, Egypt

⁴Department of Physics, Faculty of Science, Zagazig University, Zagazig, Egypt

⁵Shore Protection Authority

INTRODUCTION

The Egyptian Red Sea coast is being stressed due to over exploitation and has become very vulnerable to human related activities. Generally, the main environmental problems and threats to the Red Sea ecosystem and geosystem include recreation and tourism activities, landfilling, dredging, oil pollution, water pollution, solid waste disposal, navigation activities, phosphate shipment pollution and fishing activities. As a result of the human activities, pollution extends along the shore and is discharged to the near shore waters. Some of these pollutants may directly or indirectly be captured by bottom sediments 1,2. In addition to, Natural input of terrestrial material by wadis. Natural radionuclide in the environmental elements such as sediment and water samples contribute a significant amount of background radiation exposure to the population through inhalation and ingestion as well as through direct external exposure. Sediments are formed when rocks and/or organic materials are broken into small pieces by moving water and it plays an important role in accumulating and transporting contaminants within the geographic area3. The knowledge of specific activities or concentrations and distributions of the radionuclides in these materials are of interest since it provides useful information in the monitoring of environment radioactivity⁴⁻⁶.

The ²³⁸U series decay chain that starting by radium (²²⁶Ra) is the sources of the external and the internal radiation exposures in many human activities related to quarries, mining and oil drilling and production. In the hydrocarbon industry, oil spillage, gas flaring and drilling activities are believed to raise the natural background radiation of the environment^{7,8}. Furthermore, oil and gas, by-products of the hydrocarbon industry and the chemicals used for crude oil exploration and exploitation may contain substances that are radioactive9. The concentration and distribution pattern of ²²⁶Ra in sediment can be used to trace the radiological impact of the nonnuclear industries on the Red Sea coast. Gamma radiation emitted from natural sources (background radiation) is largely due to primordial radionuclides, mainly ²³²Th and ²³⁸U series and their decay products, as well as ⁴⁰K, which exist at trace levels in the earth's crust. The radiological impact from the natural radioactivity is due to radiation exposure of the body by gamma-rays and irradiation of lung tissues from inhalation of radon and its progeny^{10,11}. The external exposure is caused by direct gamma radiation while the inhalation of radioactive inert gases radon (222Rn, a daughter product of ²²⁶Ra) and thoron (²²⁰Rn, a daughter product of ²²⁴Ra) and their short-lived secondary products lead to the internal exposure of the respiratory tract to alpha particles 12,13.

Studying the primordial radionuclides distribution allows the understanding of the radiological implication of these elements due to the gamma-ray exposure of the body and irradiation of lung tissue from inhalation of radon and its daughters ^{14,15}.

The present study aimed to assess natural radioactivity levels of (226Ra, 232Th and 40K) for Abu Soma Bay Marine sediment. In order to evaluate the quality of the environment of Abu Soma Bay and to assess the consequences of any contamination.

MATERIALS AND METHODS

Study area: Soma Bay is wide embayment located in the western side of the Red Sea 50 km south of Hurghada City (Fig. 1a and b). The coastal area around the bay has relatively low populations accompanied relatively dense human activities in relatively small coastal horizon including, mining activities, maritimes and shipping activities, tourist activities and the related industries, fishing and ship maintaining yards. In the last three decades, the entire shoreline of Soma Bay was earmarked for tourism development, the following impacts have been recorded: Dredging, coastal infilling, marina construction, alteration of inshore current patterns as a result of breakwater construction and eutrophication¹⁶. Vegetated coastal dunes and sabkhas occupy the lowland areas at the wadi mouth namely Wadi Murrat (Fig. 1b).

The embayment contains a high diversity of bioconstructions and sedimentary settings dominated by corals such as true coral reefs (fringing reefs, patch reefs and platform reefs) and non-frame building communities¹⁶ as well as many subtidal habitats as, seagrass meadows, sand with corals, macroids, mud, hardgrounds and mangroves. Extensive fringing reef systems occupies the shallow areas inside the bay and have appeared to suffer mainly from localized impacts (high sedimentation rates, turbidity and water quality changing) due to expanding the coastal urban and industrial centres, ports and mining activities. Riegl and Piller¹⁷ concluded that the coral assemblages in northern Safaga Bay are influenced by the hydrodynamics, bottom topography, sedimentation and turbidity.

Seagrass beds were denser and better developed in the northern and western sides of the bay. Dense seagrass meadows, made up mainly by *Cymodocea* sp. and *Halophila* spp., were found in the northern and western section of the bay. A narrow strip of seagrasses mainly *Halophila* spp. intergrown with rare *Halodule uninervis*, extended south on both sides of the channel in between Safaga Island and Safaga township¹⁷.

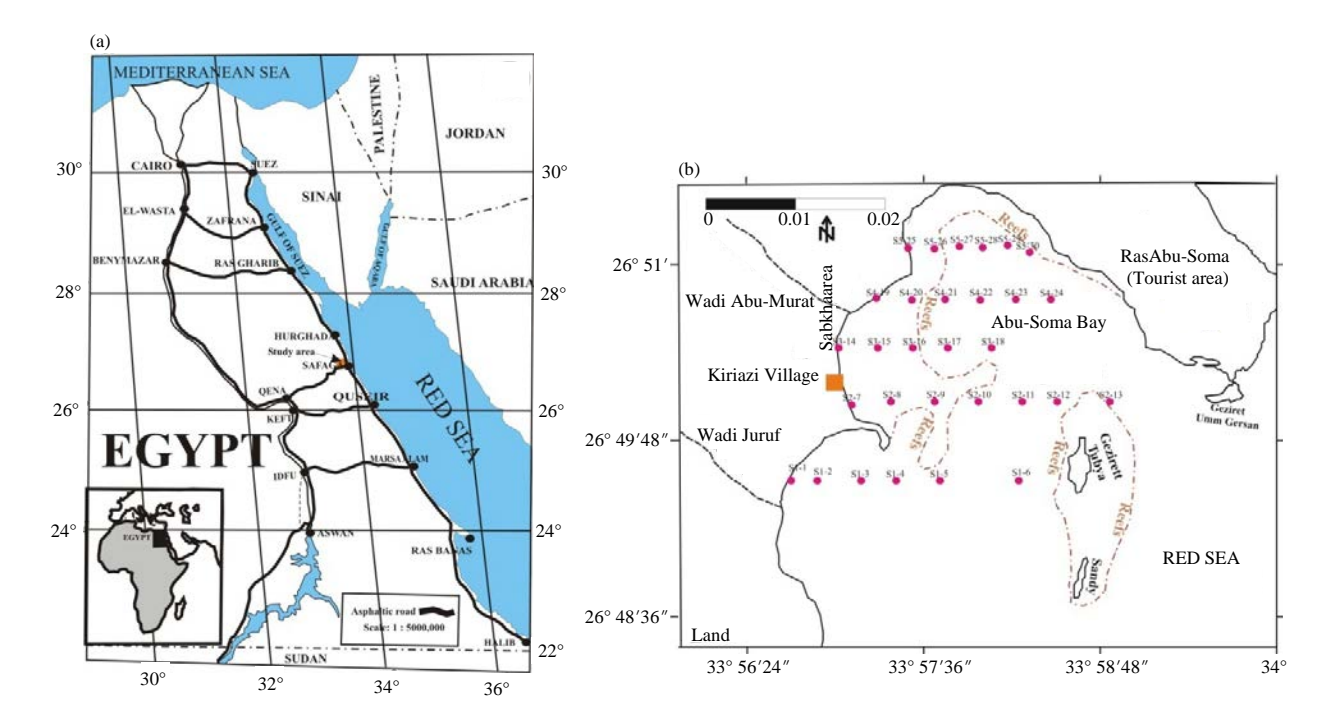


Fig. 1(a-b): (a) Study area along the Egyptian Red Sea coast, (b) Distribution of surface marine sediment samples at Abu-Soma Bay

Field works: In this study, thirty surface marine sediment samples have been collected from Abu-Soma Bay (Fig. 1), the location, depth and description of bottom characteristics of the collected samples were given in (Table 1 and Fig. 1b).

Surface marine sediments samples collected from the study area represent three different environmental feature, sabkha area, beach, intertidal zone and offshore zone until 14 m water depth. The sampling was carried out by a grab sampler and Scuba diving. The later was used in areas rich with corals where grab sampler failed to collect samples. After anchoring the boat at each station, the sampler was lowered to the sea floor and left a few seconds before being pulled back to the surface. The sediment caught in the sampler or collected by Scuba diving was placed in labeled plastic bags and returned to the laboratory^{18,19}.

Samples collection and preparation: A total of thirty marine sediment samples were collected for investigation from Abu-Soma Bay (Table 1), the samples were prepared before measurement. Each sample (about 1 kg) was dried at about 110°C to ensure that moisture is completely removed. The samples were crushed, homogenized and sieved through a 200 mesh, the optimum size to be enriched in heavy minerals. Weighted samples were placed in a polyethylene beaker of 350 cm³ volume. The beakers were completely sealed for

4 weeks to reach secular equilibrium of the decay rate between the daughter and parent nuclides of radon^{20,21}. measurements were performed spectrometry, employing a 3×3 inch scintillation NaI (TI) detector. The hermetically sealed assembly is coupled to a personal computer-multichannel analyzer (Canberra AccuSpec). A dedicated software program (Genie 2000) analyzed each measured γ -ray spectrum. To reduce γ -ray background, a cylindrical lead shield (100 mm thick) with a fixed bottom and movable cover shielded the detector. The lead shield contained an inner concentric cylinder of copper (0.3 mm thick) to absorb lead X-rays. In order to determine the background distribution in the environment around the detector, an empty sealed beaker was counted in the same manner and in the same geometry as the samples. The efficiency calibration curve was made using different energy peaks covering the range up to ~2000 keV. Measurements were performed with calibrated source samples which contain a known activity of one or more γ -ray emitters of the radionuclides 60 Co (1173.2 and 1332.5 keV), ¹³³Ba (356.1 keV), ¹³⁷Cs (661.9 keV) and ²²⁶Ra (1764.49 keV) with certified accuracies of <2%, supplied by Physikalisch-Technische-Bundesanstatt Braunschweig, Germany. Each sediment sample was measured over 12 h, as well as the background. The ²³²Th concentration was determined from the average concentrations of ²¹²Pb

Table 1: Sample location, depth and bottom facies at Abu-Soma Bay

	Position			
	Latitude	Longitude		
Sa. No.	N	 E	Depth (m)	Bottom facies
S1-1	26°50′12″	33°57′12″	1	Fine sand
S1-2	26°50′07″	33°57′16″	2	Fine sand
S1-3	26°50′07″	33°57′1″	4	biogenic sand
S1-4	26°50′07″	33°57′23″	6	biogenic sand
S1-5	26°50′07″	33°57′28″	5	biogenic sand with seagrasses
S1-6	26°50′06″	33°57′33″	4	biogenic sand with seagrasses
S2-7	26°50′17″	33°57′06″	beach	very Fine sand
S2-8	26°50′14″	33°57′12″	0.4	very Fine sand
S2-9	26°50′16″	33°57′13″	4	sandy mud
S2-10	26°50′14″	33°57′20″	5	biogenic sand
S2-11	26°50′12″	33°57′25″	6	biogenic sand with seagrasses
S2-12	26°50′11″	33°57′31″	7	biogenic sand
S2-13	26°50′10″	33°57′35″	3	biogenic sand
S3-14	26°50′33″	33°57′04″	beach	sand
S3-15	26°50′50″	33°57′08″	0.3	Fine sand
S3-16	26°50′26″	33°57′26″	3.5	biogenic sand with algae
S3-17	26°50′22″	33°57′32″	5.5	biogenic sand
S3-18	26°50′21″	33°57′36″	2.5	biogenic sand
S4-19	26°50′45″	33°57′04″	beach	medium sand
S4-20	26°50′44″	33°57′15″	0.4	Fine sand
S4-21	26°50′48″	33°57′33″	3	Fine sand
S4-22	26°50′45″	33°57′41″	9	biogenic sand
S4-23	26°50′41″	33°57′49″	11	biogenic sand
S4-24	26°50′40″	33°58′03″	8	biogenic sand
S5-25	26°51′43″	33°58′00″	beach	sand
S5-26	26°51′43″	33°58′01″	2.5	sand
S5-27	26°51′30″	33°58′03″	4.5	biogenic sand
S5-28	26°51′15″	33°58′12″	14	biogenic sand
S5-29	26°51′06″	33°58′21″	12	biogenic sand
S5-30	26°50′54″	33°58′26″	14	biogenic sand

(238.6 keV) and 228 Ac (911.1 keV) in the samples and that of 226 Ra was determined from the average concentrations of 214 Pb (351.9 keV) and 214 Bi (609.3 and 1764.5 keV) decay products. The 40 K activity was determined by the peak at the energy 1460.8 keV 19,22,23 .

The activity concentrations of the natural radionuclides in the measured samples (A_s) were computed using the following relation:

$$As(Bqkg^{-1}) = \frac{Ca}{\varepsilon p_r M_s}$$
 (1)

where, C_a is the net gamma counting rate (counts per second), ε the detector efficiency of the specific γ -ray, P_r the absolute transition probability of Gamma-decay and M_s the mass of the sample (kg)^{24,25}.

RESULTS AND DISCUSSION

Activity concentrations of ²²⁶Ra, ²³²Th and ⁴⁰K: The activity concentrations of the natural radionuclides of ²²⁶Ra, ²³²Th and

 ^{40}K in sediments samples from Abu-Soma Bay, Red Sea coast, Egypt were measured and tabulated in Table 2. The activity of ^{226}Ra ranged from 4.1 Bq kg $^{-1}$ (sample 20) to 62.0 Bq kg $^{-1}$ (sample 19). Furthermore, ^{232}Th ranged from 1.0 Bq kg $^{-1}$ (sample 20) to 55.1 Bq kg $^{-1}$ (sample 19) with a mean of 25.7 and ^{40}K ranged from 27.1 Bq kg $^{-1}$ (sample 20) to 453.4 Bq kg $^{-1}$ (sample 2) with a mean of 265.4 Bq kg $^{-1}$. The ^{40}K activity is higher than ^{232}Th and ^{226}Ra in all measured samples. The relative contribution to dose due to ^{226}R was 38.0%, followed by the contribution due to ^{232}Th and ^{40}K as 35 , 27%, respectively as shown in Fig. 2.

In order to test the correlations between ²²⁶Ra and ²³²Th, ²²⁶Ra and ⁴⁰K and ²³²Th and ⁴⁰K, the obtained concentrations of naturally occurring radionuclides were plotted in the histogram Fig. 3. It is noted that a good correlation between ²²⁶Ra and ²³²Th was observed with a correlation coefficient of 0.77, whereas a poor correlations between ²²⁶Ra with ⁴⁰K with a correlation coefficients of 0.60. According to the recommended reference level of 30, 25 and 370 Bq kg⁻¹ for ²²⁶Ra, ²³²Th and ⁴⁰K, respectively, for the World average concentrations published by UNSCEAR²⁶,

it is noted that the obtained results in most samples were lower than the recommended reference level.

The activity concentrations of ²²⁶Ra, ²³²Th and ⁴⁰K in sediment samples from the selected area was compared with those from similar investigations in other countries and summary results were given in Table 3. It is found that the mean value of ²²⁶Ra, ²³²Th and ⁴⁰K in the present study were lower than reported for sediment of Wadi El-Gemal in Egypt, but ²³²Th is found to be higher only than reported for Safaga coast, Red Sea, Egypt. The mean value of ²³²Th was found lower than reported for Wadi El-Hamra, Egypt, Pattani bay, Thailand and Wadi Abu-Shaar, Egypt. The comparison of ⁴⁰K activity concentration showing that the values of this radionuclide in the present study was higher only than Pattani bay, Thailand and Rio Formosa, Brazil and Seboul estuary Morocco and lower than other places in the Red Sea like Safaga, Wadi El Gemal, Wadi Hamata and Wadi Abu Shaar. The variations in the concentrations of the radioactivity in the

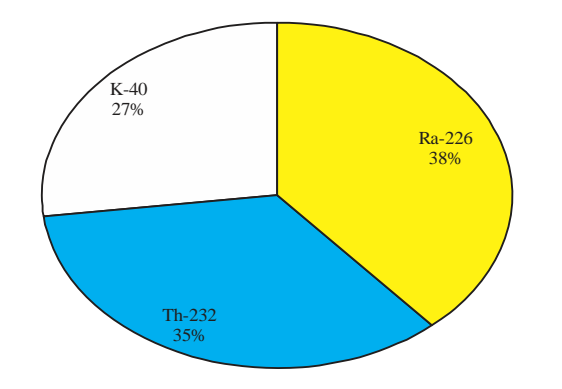


Fig. 2: Percentage contribution of ²²⁶Ra, ²³²Th and ⁴⁰K in activity concentration for Soma Bay sediments

sediment of various locations of the world depend upon the geological and geographical conditions of the area. The mean value of radionuclide concentration of ²²⁶Ra exceeded the

Table 2: Activity concentrations of (226Ra, 232Th and 40K) in the sediments samples from Abu-Soma Bay, Egypt

	Activity concentrations (Bq kg ⁻¹)			
Sample No.	²²⁶ Ra	²³² Th	⁴⁰ K	
1	8.9	7.1	117.5	
2	44.7	31.6	453.4	
3	32.7	24.0	254.4	
4	47.4	32.2	344.4	
5	45.9	31.1	361.8	
6	34.7	23.3	271.9	
7	65.3	62.4	362.2	
8	47.0	35.1	338.2	
9	40.3	30.0	225.6	
10	25.4	18.7	148.0	
11	28.6	20.0	222.7	
12	29.7	20.5	234.5	
13	26.3	17.9	200.4	
14	48.8	41.5	376.5	
15	38.8	28.1	380.8	
16	27.2	19.2	243.8	
17	32.3	21.9	251.2	
18	27.1	18.2	207.5	
19	62.0	55.1	437.0	
20	4.1	1.0	27.1	
21	30.0	21.1	267.1	
22	32.9	22.9	255.3	
23	26.2	17.6	192.1	
24	41.9	31.3	403.5	
25	29.4	19.9	182.4	
26	45.1	22.9	224.0	
27	56.6	29.0	295.3	
28	48.4	22.7	230.3	
29	46.3	22.0	231.2	
30	42.7	21.5	221.9	
average	37.2	25.7	265.4	

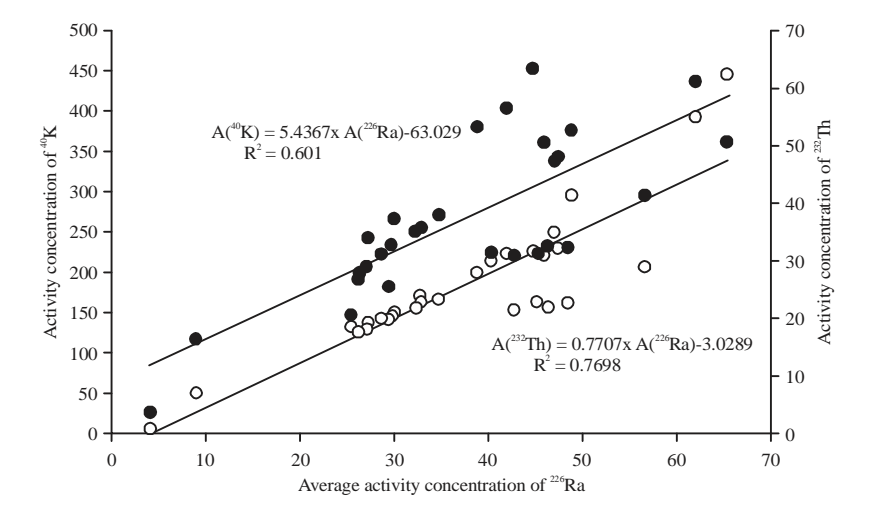


Fig. 3: Correlations between (a) ²²⁶Ra with ²³²Th, (b) ²²⁶Ra with ⁴⁰K collected from Abu-Soma Bay

Table 3: Comparison of natural radioactivity concentration (Bq kg⁻¹) in the sediments for present study with similar studies reported from different countries of the world

	Mean activity concentration (Bq kg ⁻¹)			
Countries	²²⁶ Ra	²³² Th	⁴⁰ K	References
Abu-Soma bay, Egypt.	37.2	25.7	265.4	Present study
Sofaga coast, red sea	14.3	17.0	346.5	Uosif <i>et al.</i> ¹
Rio Formosa, Brazil	21.0	-	869.0	De Paiva <i>et al.</i> ²⁷
Wadi El-Hamra, Egypt	18.5	31.1	380.0	El-Taher and Madkour ²³
Pattani bay, Thailand	4.9	55.8	183.2	Kaewtubtim et al. ²⁸
Wadi El-Gemal, Egypt	38.8	47.5	526.0	El-Taher and Madkour ²³
Amazon estuary Brazil	40.0	-	-	Neves et al. ²⁹
Seboul estuary Morocco	17.0	-	312.0	Laissaoui <i>et al</i> . ³⁰
Wadi Abu-Shaar, Egypt	24.2	35.6	418.0	El-Taher and Madkour ²³
Wadi Hamata, Egypt	35.1	42.5	491.0	El-Taher and Madkour ²³
World average	32	45	412	UNSCEAR ²⁶

Table 4: Radiological hazards (Raeq and lyr) in sediments from Abu-Soma bay
Radiological hazards

	Radiological nazards			
	Radium equivalent activity	Representative level		
Sample No.	(Ra_{eq}) Bq kg^{-1}	index (lγr)		
1	28.04	0.21		
2	124.88	0.92		
3	86.70	0.63		
4	119.97	0.87		
5	118.18	0.86		
6	89.02	0.65		
7	182.33	1.30		
8	123.16	0.89		
9	100.54	0.72		
10	63.63	0.46		
11	74.36	0.54		
12	77.16	0.56		
13	67.31	0.49		
14	137.10	0.99		
15	108.37	0.79		
16	73.33	0.54		
17	82.90	0.60		
18	69.04	0.50		
19	174.38	1.26		
20	7.59	0.06		
21	80.77	0.59		
22	85.35	0.62		
23	66.22	0.48		
24	117.67	0.86		
25	71.85	0.52		
26	95.09	0.68		
27	120.82	0.86		
28	98.57	0.70		
29	95.62	0.68		
30	90.46	0.65		
Minimum	7.59	0.06		
Maximum	182.33	1.30		
Average	94.35	0.68		

worldwide range. However, the mean value of ²³²Th and ⁴⁰K in the present study was lower than the worldwide range.

Radiological parameters

Radium equivalent activities (Raeq): The γ -ray radiation hazards due to the specified radionuclides ²²⁶Ra, ²³²Th and ⁴⁰K

were assessed by different indices. The most widely used radiation hazard index is called the radium equivalent activity. Raeq is a weighted sum of activities of the above three radionuclides based on the estimation that 370 Bq kg $^{-1}$ of 226 Ra, 259 Bq kg $^{-1}$ of 232 Th and 4810 Bq kg $^{-1}$ of 40 K produce the same g-ray dose rates. Raeq is given by the following Eq.

When the value of Raeq is 370 Bq kg $^{-1}$, this corresponds to 1 mSv y $^{-1}$. The radium equivalent concept allows a single index or number which is a widely used hazard index to describe the gamma output from different mixtures of uranium, thorium and potassium in the sediments samples from different locations. The calculated values are varied from 7.59 (sample No. 20) to 182.33 (sample No. 7) Bq kg $^{-1}$ with an average of 94.35 Bq kg $^{-1}$ (Table 4). These values are lower than the permissible maximum value of 370 Bq kg $^{-1}$ NEA-OECD1979 report.

Absorbed dose rate: The absorbed gamma dose rates DR (nGh-1) in air at 1 m above the ground surface for the uniform distribution of radionuclides were calculated based on guidelines provided by UNSCEAR²⁶.

DR
$$(nG.h^{-1}) = 0.427C_{Ra} + 0.623C_{Th} + 0.043C_{K}$$
 (3)

where, C_{Ra} , C_{Th} and C_{K} are the activity concentrations (Bq kg⁻¹) of ²²⁶Ra, ²³²Th and ⁴⁰K, respectively, in the samples. The absorbed dose rate expresses the received dose in the open air from the radiation emitted from radionuclides concentration in environmental materials. Also it is the first major step for evaluating the health risk and is expressed in Gray (Gy). The calculated total absorbed dose and annual effective dose rates of samples were tabulated in Table 5. It is observed that the total absorbed dose rate resulting from

Table 5: Dose and Annual effective gamma doses for Abu Soma marine sediments

		Annual dose rate
Sample No.	Dose rate (nGy/h)	(μSv/y)
1	13.27	16.28
2	58.68	72.00
3	40.25	49.39
4	55.71	68.36
5	55.05	67.55
6	41.47	50.88
7	82.92	101.74
8	56.99	69.92
9	46.13	56.60
10	29.24	35.88
11	34.59	42.44
12	35.92	44.07
13	31.31	38.41
14	63.30	77.66
15	50.81	62.34
16	34.29	42.07
17	38.60	47.36
18	32.14	39.43
19	80.12	98.30
20	3.62	4.44
21	37.76	46.32
22	39.70	48.71
23	30.77	37.76
24	86.72	106.41
25	3.62	4.44
26	43.16	52.95
27	46.35	56.871
28	43.96	53.93
29	44.08	54.09
30	43.68	53.59
Minimum	3.62	4.44
Maximum	86.72	106.41
Average	43.47	53.34

²²⁶Ra, ²³²Th and ⁴⁰K ranges between 3.62 (sample 20) to 86.72 (sample 24) and the average value was 43.47, which was lower than the limits as recommended by ICRP.-65 report.

Representative level index: Radiation hazards due to the specified radionuclides of 226 Ra, 232 Th and 40 K were assessed by another index called representative level index, lyr .The following equation was applied to calculate lyr for sediment samples under investigation.

$$I\gamma r = (1/150) C_{Ra} + (1/100) C_{Th} + (1/1500) C_K$$
 (4)

where, C_{Ra} , C_{Th} and C_{K} are the specific activities of 226 Ra, 232 Th and 40 K in Bq kg $^{-1}$, respectively. The l γ r varies from 0.06-1.3 with a mean value of 0.68 as shown in Table 4.

The annual effective dose equivalent (AEDE): The annual effective dose equivalent (AEDE) was calculated from the absorbed dose by applying the dose conversion factor of 0.7 Sv Gy⁻¹ with an outdoor occupancy factor of 0.2 and 0.8 for indoor UNSCEAR²⁶.

$$AEDE_{outdoor} = D (nG.h^{-1}) \times 8760 (h.y^{-1}) \times 0.7 \times (10^{3} mSv/nGy \ 10^{9}) \times 0.2$$
(5)

Equation 5 simplifies into:

$$AEDE_{outdoor} = D \times 1.226 \times 10^{-3} \text{ (mSv.y}^{-1)}$$
 (6)

$$AEDE_{indoor} = D (nG.h^{-1}) \times 8760 (h.y^{-1}) \times 0.7 (\times (10^3 \text{ mSv} / \text{nGy } 10^9)) \times 0.8$$
(7)

Equation 7 simplifies into:

$$AEDE_{indoor} = D \times 4.905 \times 10^{-3} (mSv.y^{-1})$$
 (8)

To estimate annual effective doses, account must be taken of (a) the conversion coefficient from absorbed dose in air to effective dose and (b) the indoor occupancy factor. The average numerical values of those parameters vary with the age of the population and the climate at the location considered. In the UNSCEAR³¹ Report, the Committee used 0.7 Sy Gy^{-1} for the conversion coefficient from absorbed dose in air to effective dose received by adults and 0.8 for the indoor occupancy factor, i.e. the fraction of time spent indoors and outdoors is 0.8 and 0.2, respectively. The resulting worldwide average of the annual effective dose is 0.48 mSv, with the results for individual countries being generally within the 0.3-0.6 mSv range. For children and infants, the values are about 10 and 30% higher, in direct proportion to an increase in the value of the conversion coefficient from absorbed dose in air to effective dose³².

As shown in Table 5, the annual effective dose rate ranged from 4.44-106.1 mSvy⁻¹ with a mean value of 53.34 mSvy⁻¹. The corresponding world average value is 0.41 mSvy⁻¹ of which 0.07 mSvy⁻¹ is from outdoor and 0.34 mSvy⁻¹ from indoor exposure UNSCEAR³¹. Therefore, the study area is still in the zones of normal radiation level, which leaves the sediment radioactivity there less a threat to the environment as well as the human health. Therefore, the study area is still in the zones of normal radiation level, which leaves the soil radioactivity there less a threat to the environment as well as the human health. However, this data may provide a general background level for the area studied and may also serve as a guideline for future measurement and assessment of possible radiological risks to human health in this province.

Sediments are characterized by their conservative nature, however, temporal variability should be taken into account in case of establishing the background levels. Accordingly, this data will be considered as a baseline to help in constituting the local guidelines. When local guidelines are not available,

comparisons with international ones are recommended but should be validated using local species from the local environment.

CONCLUSION

From this study, the mean and range of the concentrations of $^{226}\rm{Ra}$ and $^{232}\rm{Th}$ were 37.2 (4.1-65.3) and 25.7 (1.0-62.4) Bq kg $^{-1}$. The range of the concentrations of $^{40}\rm{K}$ in sediment samples was between 182.4 and 453.4 Bq kg $^{-1}$ with a mean value of 265.5 Bq kg $^{-1}$. The mean value of absorbed dose rate is 43.47 nGy/h, which is below the corresponding population-weight (world average) value of 65 nGyh $^{-1}$. Annual effective gamma dose were lower than the world's average. The value of Raeq activity was found to be less than 370 Bq kg $^{-1}$.

SIGNIFICANCE STATEMENT

This study discovers the natural radioactivity levels and associated radiation hazards in sediment samples collected from Ras Abu Soma along the red Sea coast. Ras Abu-Soma is located in front of one of the valleys active valleys, which is the Valley of Abu Murat. This study will be used as a baseline data for future investigations in pollution assessment and natural radioactivity mapping and could serve as a reference data for monitoring pollution studies in future.

REFERENCES

- Uosif, M.A.M., M. Hashim, S. Issa, M. Tamam and H.M. Zakaly, 2016. Natural radionuclides and heavy metals concentration of marine sediments in quseir city and surrounding areas, Red Sea Coast-Egypt. Int. J. Adv. Sci. Technol., 86: 9-30.
- El-Taher, A. and S.S. Althoyaib, 2012. Natural radioactivity levels and heavy metals in chemical and organic fertilizers used in Kingdom of Saudi Arabia. Applied Radiat. Isot., 70: 290-295.
- El-Reefy, H.I., T. Sharshar, T. Elnimr and H.M. Badran, 2010. Distribution of γ-ray emitting radionuclides in the marine environment of the Burullus Lake: II. Bottom sediments. Environ. Monit. Assess., 169: 273-284.
- 4. Harb, S., 2015. Natural radioactivity concentration and annual effective dose in selected vegetables and fruits. J. Nucl. Particle Phys., 5: 70-73.
- El-Taher, A. and M A.K. Abdelhalim, 2014. Elemental analysis of soils from Toshki by using instrumental neutron activation analysis techniques. J. Radioanal. Nucl. Chem., 300: 431-435.
- 6. El-Taher, A. and M.A.K. Abdelhalim, 2014. Elemental analysis of limestone by instrumental neutron activation analysis. J. Radioanal. Nucl. Chem., 299: 1949-1953.

- 7. Alashrah, S. and A. El-Taher, 2016. Assessment of natural radioactivity level and radiation hazards in soil samples of Wadi Al-Rummah Qassim province, Saudi Arabia. J. Environ. Biol., 37: 985-591.
- 8. El-Taher, A. and J.H. Al-Zahrani, 2014. Radioactivity measurements and radiation dose assessments in soil of Al-Qassim region, Saudi Arabia. Indian J. Pure Applied Phys., 52: 147-154.
- Avwiri, G.O., Y.E. Chad-Umoren, P.I. Enyinna and E.O. Agbalagba, 2008. Occupational radiation profile of oil and gas facilities during production and off- production periods in Ughelli, Nigeria. Factia Univ. Ser.: Working Living Environ. Prot., 6: 11-19.
- El Mamoney, M.H. and A.E.M. Khater, 2004. Environmental characterization and radio-ecological impacts of non-nuclear industries on the Red Sea coast. J. Environ. Radioact., 73: 151-168.
- 11. El-Taher, A., 2012. Elemental analysis of granite by Instrumental Neutron Activation Analysis (INAA) and X-ray Fluorescence Analysis (XRF). Applied Radiat. Isot., 70: 350-354.
- 12. El-Taher, A., 2012. Assessment of natural radioactivity levels and radiation hazards for building materials used in Qassim Area, Saudi Arabia. Rom. J. Phys., 57: 726-735.
- 13. El-Taher, A., 2010. Determination of chromium and trace elements in El-Rubshi chromite from Eastern Desert, Egypt by neutron activation analysis. Applied Radiat. Isot., 68: 1864-1868.
- 14. El-Taher, A., 2010. Elemental content of feldspar from Eastern Desert, Egypt, determined by INAA and XRF. Applied Radiat. Isot., 68: 1185-1188.
- 15. Uosif, M.A.M., A. El-Taher and A.G. Abbady, 2008. Radiological significance of beach sand used for climatotherapy from Safaga, Egypt. Radiat. Prot. Dosim., 131: 331-339.
- El-Taher, A. and S. Makhluf, 2010. Natural radioactivity levels in phosphate fertilizer and its environmental implications in Assuit governorate, Upper Egypt. Indian J. Pure Applied Phys., 48: 697-702.
- 17. Riegl, B. and W.E. Piller, 1997. Distribution and environmental control of coral assemblages in Northern Safaga Bay (Red Sea, Egypt). Facies, 36: 141-162.
- 18. Rasser, M. and W.E. Piller, 1997. Depth distribution of calcareous encrusting associations in the Northern Red Sea (Safaga, Egypt) and their geological implications. Proc. 8th Int. Coral Reef Symp., 1: 743-748.
- Madkour, H.A., A. El-Taher, A.N. El-Hagag Ahmed, A.W. Mohamed and T.M. El-Erian, 2012. Contamination of coastal sediments in El-Hamrawein Harbour, Red Sea, Egypt. J. Environ. Sci. Technol., 5: 210-221.
- 20. Madkour, H.A., M.A.K. Abdelhalim and A. El-Taher, 2013. Assessment of heavy metals concentrations resulting natural inputs in Wadi El-Gemal surface sediments, Red Sea coast. Life Sci. J., 10: 686-694.

- 21. Abbady, A.G.E., M.A.M. Uosif and A. El-Taher, 2005. Natural radioactivity and dose assessment for phosphate rocks from Wadi El-Mashash and El-Mahamid Mines, Egypt. J. Environ. Radioact., 84: 65-78.
- 22. El-Gamal, A., S. Nasr and A. El-Taher, 2007. Study of the spatial distribution of natural radioactivity in the upper Egypt Nile river sediments. Radiat. Meas., 42: 457-465.
- 23. El-Taher, A. and H.A. Madkour, 2011. Distribution and environmental impacts of metals and natural radionuclides in marine sediments in-front of different wadies mouth along the Egyptian Red Sea Coast. Applied Radiat. Isot., 69: 550-558.
- 24. El-Taher, A. and H.A. Madkour, 2013. Texture and environmental radioactivity measurements of Safaga sand dunes. Indian J. Geo-Mar. Sci., 42: 35-41.
- El-Taher, A. and H.A. Madkour, 2014. Environmental and radio-ecological studies on shallow marine sediments from harbour areas along the Red Sea coast of Egypt for identification of anthropogenic impacts. J. Isotopes Environ. Health Stud., 50: 120-133.
- UNSCEAR., 2000. United Nations scientific committee on the effect of atomic radiation. Sources and Effects of Ionizing Radiation. Report to the General Assembly. United Nations, New York.

- De Paiva, J.D.S., E.E. Sousa, E.E.G. de Farias, A.M. Carmo, E.M. Souza and E.J. De Franca, 2016. Natural radionuclides in mangrove soils from the State of Pernambuco, Brazil. J. Radioanal. Nucl. Chem., 307: 883-889.
- 28. Kaewtubtim, P., W. Meeinkuirt, S. Seepom and J. Pichtel, 2017. Radionuclide (²²⁶Ra, ²³²Th, ⁴⁰K) accumulation among plant species in mangrove ecosystems of Pattani Bay, Thailand. Mar. Pollut. Bull., 115: 391-400.
- 29. Neves, P.A., P.A. de Lima Ferreira, M.C. Bicego and R.C.L. Figueira, 2014. Radioanalytical assessment of sedimentation rates in Guajara bay (Amazon Estuary, N Brazil): A study with unsupported ²¹⁰Pb and ¹³⁷Cs modeling. J. Radioanal. Nucl. Chem., 299: 407-414.
- Laissaoui, A., J.L. Mas, S. Hurtado, N. Ziad, M. Villa and M. Benmansour, 2013. Radionuclide activities and metal concentrations in sediments of the Sebou Estuary, NW Morocco, following a flooding event. Environ. Monit. Assess., 185: 5019-5029.
- UNSCEAR., 1993. United Nations scientific committee on the effects of atomic radiation. Sources and Effects of Ionizing Radiation. Report to the General Assembly with Scientific Annexes. United Nations, New York, USA.
- 32. Uosif, M.A.M. and A. El-Taher, 2008. Radiological assessment of Abu-Tartur phosphate, Western desert Egypt. J. Radiat. Prot. Dosimetry, 130: 228-235.a